Sensor Orientation Invariant Mobile Gait Biometrics

Yu Zhong Yunbin Deng

AIT, BAE Systems
6 New England Executive Park
Burlington, MA 01803-5012 USA
{yu.zhong,yunbin.deng}@baesystems.com

Abstract

Accelerometers and gyroscopes embedded in mobile devices have shown great potential for non-obtrusive gait biometrics by directly capturing a user's characteristic locomotion. Despite the success in gait analysis under controlled experimental settings using these sensors, their performance in realistic scenarios is unsatisfactory due to data dependency on sensor placement. In practice, the placement of mobile devices is unconstrained. In this paper, we propose a novel gait representation for accelerometer and gyroscope data which is both sensor-orientation-invariant and highly discriminative to enable high-performance gait biometrics for real-world applications. We also adopt the i-vector paradigm, a state-of-the-art machine learning technique widely used for speaker recognition, to extract gait identities using the proposed gait representation. Performance studies using both the naturalistic McGill University gait dataset and the Osaka University gait dataset containing 744 subjects have shown dominant superiority of this novel gait biometrics approach compared to existing methods.

1. Introduction

Gait is the special pattern of human locomotion. It is fairly unique to an individual due to one's specific muscular-skeletal bio-mechanism. Humans can often effortlessly recognize acquaintances by the way they walk or jog. However, as a behavioral biometric, gait may also be affected by transient factors such as tiredness, sickness, emotions, etc. In addition, external factors such as clothes, shoes, carried loads, and ground characteristics influence gait as well [2].

Automatic gait biometrics, which studies gait using sensory data, has been an active research area receiving increasing attention over the years [4][15][18][25]. Similar to fingerprint and iris biometrics [13], gait biometrics can be performed for two purposes [14]:

- identification, where a gait is compared to a database of enrolled gaits with known identities to determine whom the unknown gait belongs to, and
- authentication, where a gait is compared to the enrolled gait data of a known person to validate his or her identity.

In the past decade, accelerometers have been intensely researched for gait [6][20] and activity [3] analysis. More recently, gyroscopes have also been explored for body motion analysis [1][21]. These sensors directly measure locomotion when worn on a human body, opening possibilities for highly accurate gait biometrics. With the ubiquity of mobile devices embedded with accelerometers and gyroscopes, motion data can be collected continuously and effortlessly for unobtrusive gait-based authentication and identification as a mere consequence of a user carrying the mobile device around.

Despite a surge in research efforts, gait biometrics using accelerometers and gyroscopes remain a challenge for practical applications due to data dependency on sensor placement: accelerations and rotations are measured along the sensor axis. The measurements change with sensor orientation even when body motion stays the same. Most existing research is conducted in fixed laboratory settings with restricted sensor placement to bypass this problem, and is vulnerable in real-world conditions where the placement of mobile devices is casual and even arbitrary. Although promising results have been reported in well-controlled studies on gait biometrics using accelerometers, there is still a large performance gap between laboratory research and real-world applications.

In this paper, we address the challenge of sensor orientation dependency in the collection of acceleration and rotation data. To do so, we compute invariant gait representations that are robust to sensor placement while preserving highly discriminative temporal and spatial gait dynamics and context. We advance the state of the art for gait biometrics using accelerometers and gyroscopes by:

1. Directly computing gait features invariant to sensor rotation for robust matching and classification, unlike many existing works which make unrealistic assumptions of fixed sensor placement.
2. Capturing the gait dynamics and motion interactions within gait cycles to be highly discriminative.
3. Adopting the i-vector identity extraction, a prominent speaker authentication approach, for gait biometrics.

This research was developed partially with funding from the Defense Advanced Research Projects Agency (DARPA). The views expressed are those of the author(s) and do not reflect the official policy or position of the Department of Defense or the U.S. Government. Approved for Public Release, Distribution Unlimited.

4. Sensibly fusing the accelerometer and gyroscope sensors for gait biometrics, and demonstrate for the first time that gyroscopes can be used to boost the gait biometrics accuracy using accelerometers.
5. Enabling high performance realistic gait biometrics for a large population through a combination of the above advancements.

The remainder of the paper is structured as follows. Section 2 surveys related work. Section 3 introduces a novel invariant gait representation. Section 4 describes the i-vector based gait classification procedure. Section 5 presents gait biometrics experiments and performance studies. Section 6 draws conclusions, discusses the limits, and presents areas for future research.

2. Related work

Accelerometer based gait and activity analysis has been a popular research area since the pioneering work by Mantyjarvi et al. a decade ago [20]. Early work used multiple motion sensors attached to human body parts to analyze their movements and bio kinematics. Later, data from a single sensor at a fixed position such as the feet, hips, or waist was also exploited [10]. With the proliferation of smart phones equipped with advanced sensors, there has been a surge of research interest on the use of accelerometers in commercial off-the-shelf (COTS) mobile devices for activity and gait classification [9] [11][17][26]. Unlike dedicated sensors used in earlier research, accelerometer signals in mobile devices are usually irregularly sampled at a relatively low frame rate for power conservation and efficient resource sharing.

Commonly used 3-axis accelerometers capture accelerations along three orthogonal axes of the sensor. Given a multivariate time series of the acceleration data, feature vectors are usually extracted for signal windows corresponding to each detected gait cycle [7] [27] or for windows of a pre-specified size [17]. These windowed signals are compared and matched based on template matching [7], using either the correlation method or dynamic time warping. Alternatively, statistical features including mean, standard deviations, and time span between peaks in windows [17], histograms [17][20], entropy, higher order moments [10], and cumulants [26] in spatial domain are also used. FFT and wavelet coefficients [20][27] in frequency domains are also studied to compare longer sequences. Classifiers including nearest neighbor classifier, SVM [27], and Kohonen self-organizing maps [11] have been investigated. In some cases, preprocessing such as weighted moving average [7] is applied to suppress noise in the raw sensory data.

Most existing researches are conducted in well controlled laboratory settings: there are strict constraints on where and how the sensors are placed to reduce variation and noise in the data. In some cases the sensors are placed in a specific way so that intuitive meanings can be assigned to the data components and be exploited for gain analysis. For example, [20] exploited a specific sensor placement to omit the left-right motion component, which is deemed less discriminative.

For practical applications, it is unrealistic to assume fixed placement of the sensor. Mobile devices are often carried casually in pockets or hands without constraints in orientation. Since the same locomotion may result in completely different measurements with changing sensor orientation, it is essential to compute gait biometrics robust to sensor rotation for realistic scenarios.

Magnitude sequences of accelerometer measurements have been popular in use due to their invariance to sensor orientation changes ([9][22][27]). However, using the univariate resultant series of the raw 3D multivariate series results in information loss and ambiguity artifacts undesirable for highly accurate gait biometrics.

Mantyjarvi et al. [20] used both principal component analysis (PCA) and independent analysis (ICA) to discover "interesting directions" for computing gait features for activity analysis. Unfortunately, the underlying assumption of identical data distributions for both training and testing data are unlikely to hold for realistic applications.

Iso et al. [12] approached this challenge by augmenting the training set with simulated data at multiple sensor orientations via artificially rotating available training data. In their approach, the significant artificial sampling needed to tessellate 3D rotational space creates an unbearable computational and storage burden with the additional risk of degraded classifier performance. In [16], orientation invariant features were extracted using the power spectrum of the time series. However, it suffered shortcomings common to frequency domain methods: loss of temporal locality and precision, and vulnerability to drifts in gait tempo.

Sprager et al. [26] used a co-built-in gyroscope sensor to calibrate accelerometer data to the upright posture in order to reduce the influence of noise in sensor orientation. Their approach requires calibration prior to every data collection, expects the sensor not to rotate during data collection, relieves only noise in the vertical direction, and makes unrealistic assumptions that all poses are upright.

These studies paint a picture of drastic degradation in gait recognition performance in more relaxed scenarios. Even with the new invariant features, accuracy of approximately 50% was reported in [16]. Accuracies between 27% and 63% were reported in [9]. On the other hand, accuracies in the high 90 percentages are often achieved in more controlled scenarios. Although each study used its own dataset and evaluation standards and the numbers are not directly comparable, the consistent

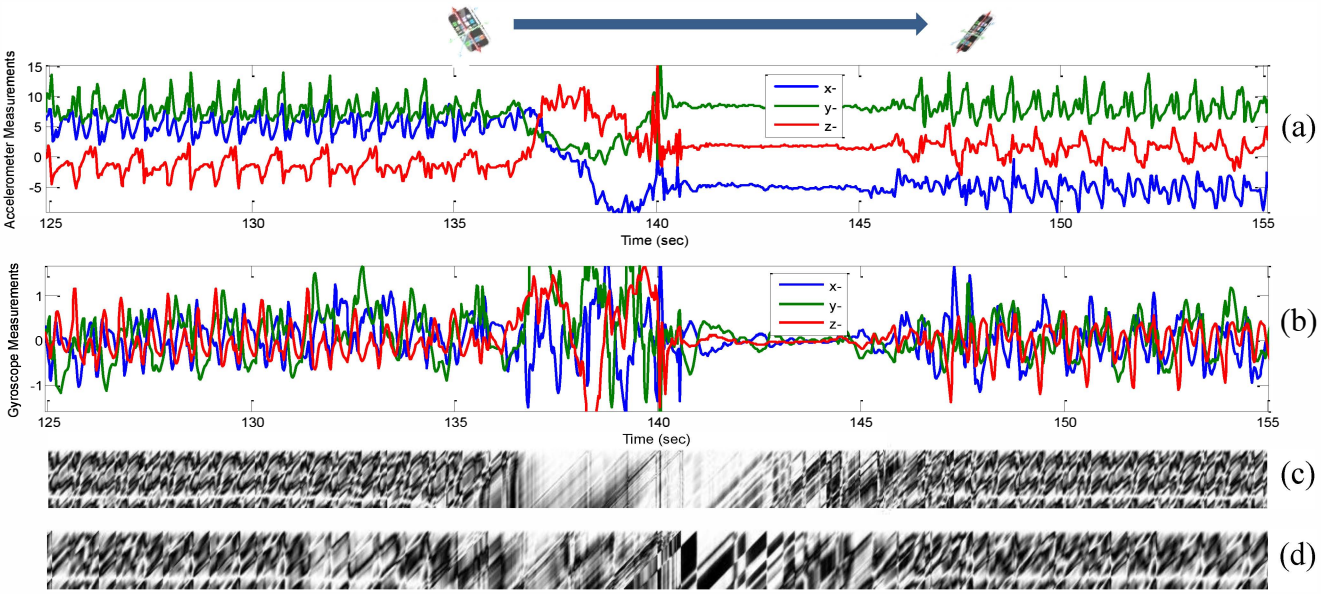

Figure 1. (a) x-, y-, and z- acceleration components from an accelerometer embedded in a mobile phone carried by a walking subject; (b) x-, y-, and z- rotation rate measurements from the embedded gyroscope. Both sensors capture distinguishing locomotion patterns characteristic of a person's gait. However, as the subject re-positioned the sensor (in the middle of the sequence), the captured gait patterns change drastically due to data dependency on sensor orientation; (c) the corresponding gait dynamics image (GDI) feature representation for the raw acceleration sequence in (a); (d) the corresponding GDI for the raw gyro sequence in (b). The gravity component is removed from the acceleration time series before the computation of GDIs. The GDIs are invariant to sensor orientation and thus show much better consistency before and after the sensor re-positioning.

large gap in performance does highlight the challenge for realistic gait biometrics using orientation-dependent motion sensors. For a mobile device based gait biometrics system to succeed in real world applications, it is crucial to address the variations in sensor orientation due to casual handling of mobile devices.

3. Invariant gait representation

One of the major challenges for mobile device based gait biometrics is the data dependency on sensor orientation. As shown in Figure 1 (a) and (b), the accelerometer and gyroscope measurement patterns collected using a mobile phone before and after a sensor rotation, differ drastically, making gait matching a challenging task. For realistic mobile gait biometrics, the device placement is casual and unconstrained. It is essential to extract features that are robust to the sensor rotation.

We approach the challenge caused by variation in sensor orientation by exploring gait features that characterize the distinguishing locomotion signature while staying invariant to sensor orientation. We note that although the individual acceleration data does depend on sensor placement, it is possible to extract relationships between a pair of observations from one sensor that do not. Subsequently, we can compute features using these pairwise interactions inside each gait cycle to capture the gait dynamics, resulting in discriminative and robust representations for gait analysis.

3.1. Orientation invariants for accelerometer data

Given two 3D acceleration measurement vectors at times t_1 and t_2, $\overrightarrow{A(t_1)} = [x(t_1) \quad y(t_1) \quad z(t_1)]^t$ and $\overrightarrow{A(t_2)} = [x(t_2) \quad y(t_2) \quad z(t_2)]^t$, by an accelerometer with reference frame OXYZ, assume these forces are also captured by a second accelerometer with a reference frame OX'Y'Z': $\overrightarrow{A'(t_1)} = [x'(t_1) \quad y'(t_1) \quad z'(t_1)]^t$ and $\overrightarrow{A'(t_2)} = [x'(t_2) \quad y'(t_2) \quad z'(t_2)]^t$. Let the rotation between the two sensors be R. We have $\overrightarrow{A'(t_1)} = R\overrightarrow{A(t_1)}$ and $\overrightarrow{A'(t_2)} = R\overrightarrow{A(t_2)}$. Although the raw acceleration readings depend on the sensor orientation, we are able to extract orientation invariant features using a pair of motion vectors at times t_1 and t_2:

$$\begin{aligned} < \overrightarrow{A'(t_1)}, \overrightarrow{A'(t_2)} > &= < R\overrightarrow{A(t_1)}, R\overrightarrow{A(t_2)} > \\ &= \overrightarrow{A(t_2)}^T R^T R \overrightarrow{A(t_1)} \\ &= < \overrightarrow{A(t_1)}, \overrightarrow{A(t_2)} > \end{aligned} \qquad \textbf{Eq. 1}$$

We can thus define the inner product invariant to sensor rotation:

$$I_{inp}\left(\overrightarrow{A(t_1)}, \overrightarrow{A(t_2)}\right) = < \overrightarrow{A(t_1)}, \overrightarrow{A(t_2)} > \quad \textbf{Eq. 2}$$

This invariant quantity is related to the projection of one acceleration vector on the other, which stays the same regardless of the choice of the reference frame. In the special case when $t_1 = t_2$, we have:

$$< \overrightarrow{A(t)}, \overrightarrow{A(t)} >= \|x(t)^2 + y(t)^2 + z(t)^2\|,$$

which is the commonly used magnitude series.

From these invariants, we can derive additional invariant features with normalizing effects. Among them is the normalized cosine similarity measure:

$$I_{nc}\left(\overrightarrow{A(t_1)}, \overrightarrow{A(t_2)}\right) = \frac{<\overrightarrow{A(t_1)}, \overrightarrow{A(t_2)}>}{\left\|\overrightarrow{A(t_1)}\right\|\left\|\overrightarrow{A(t_2)}\right\|} \quad \textbf{Eq. 3}$$

Intuitively, this invariant is the cosine of the angle between two 3D acceleration vectors. It remains the same for all reference frames that are static with respect to each other.

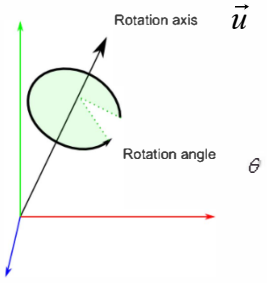

Figure 2. Alternative rotation representation.

3.2. Orientation invariants for gyroscope data

Gyroscopes measure the rotation (or rotation rate) about the sensor's axis, which is a different physical quantity from the linear accelerations measured by accelerometers. However, we can still extract orientation invariants from a pair of raw gyro sensory data using appropriate rotation representations. Instead of using rotation matrix or Euler angles, a 3D rotation (rate) at time t can alternatively be uniquely represented using a 3D rotation axis vector $\vec{u}(t)$ and a scalar rotation angle $\theta(t)$ around the axis (Figure 2). With this rotation representation, the angle $\theta(t)$ is invariant to the choice of reference coordinate system. The coordinates of rotation axis $\vec{u}(t)$, on the other hand, does depend on the choice of reference frame. Yet, we can extract reference invariant features using a pair of 3D rotation vectors $\vec{u}(t_1)$ and $\vec{u}(t_2)$ obtained at time t_1 and t_2 as follows:

$$< \overrightarrow{u'(t_1)}, \overrightarrow{u'(t_2)} > = < R\overrightarrow{u(t_1)}, R\overrightarrow{u(t_2)} > = < \overrightarrow{u(t_1)}, \overrightarrow{u(t_2)} > \quad \textbf{Eq. 4}$$

In other word, although the rotation (or rotation rate) axes depend on the sensor orientation, the inner product between a pair of the 3D rotation axis vectors does not. This invariant quantity is related to the angle between the two axes, which stays the same regardless of the choice of the reference frame.

For 3-axis rate gyroscopes, let $\overrightarrow{\omega(t)} = [\omega_x(t) \quad \omega_y(t) \quad \omega_z(t)]^T$ be the output of measured rotation rate about the x-, y-, z- axes expressed in *rad/s*. According to the theory on Direction Cosine Matrix IMU [24], for a small time *dt* , the combination of three small rotations about the x-, y-, z-axes characterized by angular rotation vectors $\overrightarrow{\omega_x(t)}$, $\overrightarrow{\omega_y(t)}$, $\overrightarrow{\omega_z(t)}$, where $\overrightarrow{\omega_x(t)} = [\omega_x(t) \quad 0 \quad 0]^T$, $\overrightarrow{\omega_y(t)} = [0 \quad \omega_y(t) \quad 0]^T$, $\overrightarrow{\omega_z(t)} = [0 \quad 0 \quad \omega_z(t)]^T$, is approximately equivalent to one small simultaneous rotation characterized by angular rotation vector $\overrightarrow{\omega(t)} = [\omega_x(t) \quad \omega_y(t) \quad \omega_z(t)]^T$, which is a rotation around the axis defined by $[\omega_x(t) \quad \omega_y(t) \quad \omega_z(t)]^T$, with an angle equal to the magnitude $\|[\omega_x(t) \quad \omega_y(t) \quad \omega_z(t)]^T\|$.

From previous discussion, we have established that the magnitude of $\overrightarrow{\omega(t)}$, which is the rotation angle around the 3D rotation axis, is invariant to the sensor axis, and the inner product of a pair of $\overrightarrow{\omega(t)}$ is also invariant to the sensor reference frame. Consequently, we can compute invariant features for a pair of angular rate readings $\overrightarrow{\omega(t_1)} = [\omega_x(t_1) \quad \omega_y(t_1) \quad \omega_z(t_1)]^T$ and $\overrightarrow{\omega(t_2)} = [\omega_x(t_2) \quad \omega_y(t_2) \quad \omega_z(t_2)]^T$ from gyroscopes:

$$I_{inp}(t_1, t_2) = < \overrightarrow{\omega(t_1)}, \overrightarrow{\omega(t_2)} > \quad \textbf{Eq. 5}$$

In the special case when $t_1 = t_2$, we have

$$I_{inp}(t, t) = < \overrightarrow{\omega(t)}, \overrightarrow{\omega(t)} > = \left\|\overrightarrow{\omega(t)}\right\|.$$

We also extract normalized cosine similarity invariants:

$$I_{nc}(t_1, t_2) = \frac{<\overrightarrow{\omega(t_1)}, \overrightarrow{\omega(t_2)}>}{\left\|\overrightarrow{\omega(t_1)}\right\|\left\|\overrightarrow{\omega(t_2)}\right\|} \quad \textbf{Eq. 6}$$

3.3. Gait dynamics images

We exploit these invariant motion interactions to extract features that characterize the locomotion dynamics and which are robust to variations in sensor orientation. Given a 3D acceleration or rotation rate time series of size n sampled at regular time intervals $\{\overrightarrow{A(1)}, \overrightarrow{A(2)}, \overrightarrow{A(3)}, \ldots, \overrightarrow{A(n-1)}, \overrightarrow{A(n)}\}$, we define a two dimensional matrix which we call Gait Dynamics Image (GDI) to capture invariant motion dynamics over time and interactions within each gait cycle. Let the invariant feature computed using data vectors $\overrightarrow{A(t_1)}$ and $\overrightarrow{A(t_2)}$ be $I(t_1, t_2)$, using either Eq. 2 or Eq. 3 for acceleration measurements, and Eq. 5 or Eq. 6 for rotation measurements. The GDI is defined as follows:

$$GDI(i, j) = I(j, i + j - 1), \quad \textbf{Eq. 7}$$
$$i = 1, \ldots, l \text{ and } j = 1, \ldots, n - l + 1,$$

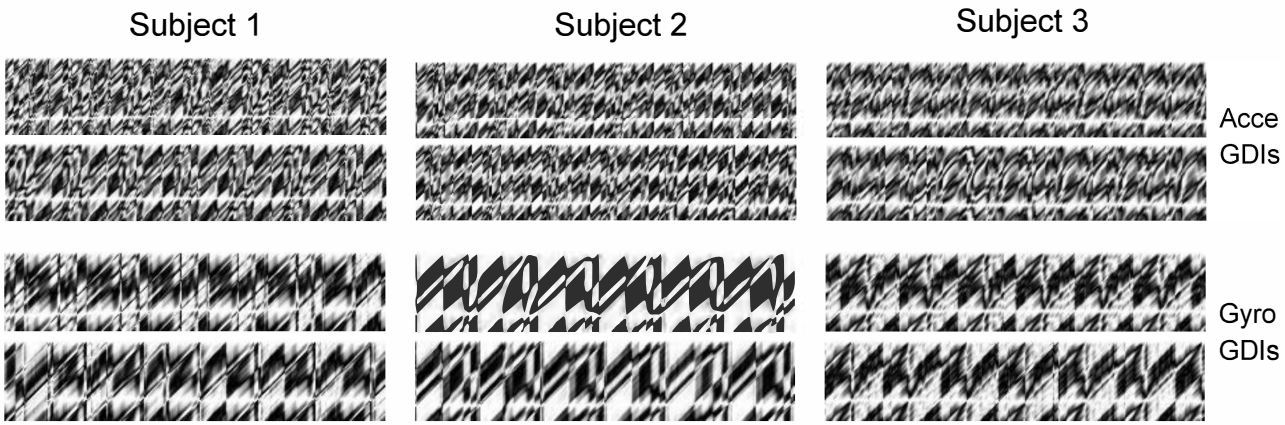

Figure 3. Gait dynamics images exhibit good intra-subject consistency and notable inter-subject distinctions despite of sensor orientation variations.

where l is the range of the time delay for concerning pairwise motion interactions, for which we choose to encode context within a typical gait cycle.

Gait Dynamics Images encode rich dynamics and context information characterizing the unique gait of an individual. The ith row of the GDI contains all pairwise interactions of time delay $i-1$ over time, while the jth column consists of interactions between the motion at time j and all its successors up to time lag $l-1$ to capture local context. In particular, the first row of the inner product GDI (Inp GDI) image, which are the inner products of observation pairs with time lag 0, corresponds to the magnitude sequence. The magnitude sequence has been shown to be advantageous to the raw component acceleration features in cell phone based gait ID studies [27], and has been often used in existing research to handle the variations in sensor placement. The remaining rows contain the interactions at varying time lags that contribute to additional discriminating information of gait dynamics. This makes GDIs extremely powerful representations for gait biometrics.

The cosine similarity GDIs (NC GDI) can be considered a normalized form of the inner product GDIs by taking out the effects of the magnitudes. These GDIs only depend on the angles between the observation vectors. This normalization may improve the robustness to noisy magnitudes in the data. In summary, the GDI, although built on the sensor rotation dependent raw acceleration measurements, achieves a view invariant representation of the governing dynamics in the original multivariate time series for robust gait analysis. Furthermore, it preserves the local interactions and contextual information within each gait cycle essential for discriminative motion analysis to enable highly accurate gait biometrics. We show in Figure 1 (c) and (d) the corresponding cosine similarity GDIs for the raw acceleration measurements in (a) and rotation rate measurements in (b). As expected, the GDIs exhibit much better consistencies between the two collections than the raw time series. We show in Figure 3 the cosine similarity GDIs for three subjects from two sessions. As one can see, GDIs exhibit good intra-subject consistency and notable inter-subject distinctions despite of sensor orientation variations.

In addition to invariance to sensor orientation changes, GDIs are also invariant to symmetry transform or any concatenation of symmetry and rotation transforms in the motion measurements. This is apparent as both Eq. 1 and Eq. 4 hold if we replace the rotation matrix R with any symmetry transform matrix or concatenations of rotation and symmetry transforms. As the laterally symmetric human anatomy typically creates symmetric locomotion for the left and right sides of the body, it is possible to match GDIs from a phone placed in one pocket to GDIs from phones in the opposite side pocket, thus further ease the sensor placement constraint.

GDIs encode both dynamics for the time series and the local interactions. Given the irregular periodic input locomotion time series, gait dynamics images also display quasi-periodicity in both the time and time lag domains with the period approximating the length of a gait cycle.

As shown in Figure 3, these GDI images, when the time lag coincides with the length of the local gait cycle, the GDI features have high values as signals repeat themselves. This is reflected by horizontal lines of high similarity measurements in both GDIs, starting with the first row, repeating at the length of a gait cycle. Gait cycles can be estimated by fitting smooth horizontal curves across the image which maximizes the overall intensities. Due to the quasi-periodic nature of gait and the repetitive pattern in GDIs, we set $\boldsymbol{l}$ to be a little more than the length of average gait cycles to preserve all contexts within a gait cycle when computing GDIs.

4. Gait classification using GDIs and I-vector

We adopt the i-vector model that is commonly used for speaker verification to classify GDIs for gait biometrics. Despite their different application domains, voice biometrics and gait biometrics are similar in nature as both needs to extract subject specific signatures from sensory data corrupted with variations from various irrelevant sources. The identity vector (i-vector) extraction method using total variability factor analysis [5] provides an appealing solution to gait identity extraction using GDIs.

In the following we outline the i-vector extraction procedure. Interested readers should refer to [5] for more details. The i-vector modeling for user authentication consists of three major steps:

1. Build a universal background model (UBM) using a Gaussian mixture model (GMM) by pooling all or a subset of the feature vectors from the training data set. Note that the raw GDI features are enhanced with additional delta GDI features, just like delta speech features used in speaker recognition.
2. Given the trained UBM (Ω), we compute a supervector for each enrollment or authentication gait GDI feature sequence of L frames $\{y_1, y_2, \cdots, y_L\}$, where each frame is a feature vector of dimension F:
   a. the posterior probability (N_c) and Baum-Welch statistics ($\tilde{F}_c$) for each Gaussian component are computed as:
   $N_c = \sum_{t=1}^{L} P(c|y_t, \Omega)$, and
   $\tilde{F}_c = \sum_{t=1}^{L} P(c|y_t, \Omega)(y_t - m_c)$,
   where m_c is mean vector for Gaussian component c.
   b. The supervector M is obtained by concatenating $\tilde{F}_c$ for all Gaussian components to form a vector of fixed dimension $C \cdot F$ for an input sequence of arbitrary length L.
3. Conduct factor analysis in the supervector space using a simplified linear model:
   $M = m + Tw$
   where m is a subject independent component, T is a low rank rectangular matrix, and w is the i-vector. The training process learns the total variability matrix T and a residue variability covariance matrix Σ. The i-vector is then computed as:
   $w = (I + T^t \Sigma^{-1} N T)^{-1} T^t \Sigma^{-1} M$,
   where N is a diagonal matrix consisting of diagonal blocks of $N_c I$.

Once an i-vector is extracted for each gait sequence, the similarity between two gait sequences is then computed as the cosine distance between their corresponding i-vectors:

$$d(w_1, w_2) = \frac{<w_1, w_2>}{\|w_1\| \|w_2\|}$$

5. Performance analysis

We have conducted performance analysis of our gait biometrics algorithm using two publicly available gait biometrics datasets.

5.1. McGill University naturalistic gait dataset

The goal of this experiment is to investigate the effectiveness of GDIs for robust gait biometrics. We used the real-world dataset for gait recognition from McGill University [8] due to its analogy to realistic gait biometrics using mobile devices. Data were collected using HTC Nexus One phones on two different days with little constraint on the placement of the phone except that it was put in a pocket on the same side of a subject during the two data collections.

We extract GDIs corresponding to 50 seconds of raw signals with a time lapse of up to 1.2 seconds. A simple correlation based classification method is used to assess the effectiveness of the GDI representations. The similarity between two gait sequences is computed by aggregating peak correlation coefficients between GDI windows of 2.4 seconds. Nearest neighbor classifier is used. We compare the recognition accuracy using the GDIs to a baseline using only the magnitude series (which is the first row of the inner product GDI) because of its popularity in existing studies and superior performance to other features [27]. Two scenarios: 1) training and testing using non-overlapping data collected on the same day, and 2) training and testing using data from separate days, are examined. Obviously the latter is more challenging as the attires, carried loads, shoes, and most importantly the phone placements are all subjected to change, in addition to the variations in the same-day scenario.

Approach	Identification accuracies	
	Same day	Separate days
Magnitude (baseline)	67.5%	32.5%
Inp GDI	87.5%	61.3%
NC GDI	85.0%	66.3%

Table 1. Gait ID accuracy on the McGill University gait dataset using Gait Dynamics Images.

Table 1 shows the accuracies for the gait identification algorithms. Although both the magnitude series and GDIs are robust to orientation variations, GDIs contain much more information on context and interactions in gait cycles, allowing them to offer powerful discrimination and perform significantly better than the magnitude features. This advantage is even more drastic for the challenging separate–day scenario with more variations, where we obtain an accuracy of 66.3% - more than doubling the accuracy using magnitude features. Though all methods performed worse for the separate-day scenario, the

methods using GDIs degraded much more gracefully thanks to their rich discriminating gait dynamics.

5.2. Osaka University largest gait dataset

The McGill dataset is a realistic dataset. However, it only includes accelerometer data with 20 subjects. We thus conducted experiments on the largest publicly available gait dataset - the Osaka Univ. dataset [21] which consists of 744 subjects with both gyroscope and accelerometer data. In this dataset, each subject has two walking sequences- one for training and one for testing.

We apply the i-vector technology to the GDI feature sequence for gait authentication. The UBM was modeled by a GMM of 800 components and the final i-vector was 60 and 40 dimensions for the accelerometer and the gyroscope modality, respectively. The authentication was based on the cosine similarity of i-vectors. We conducted exhaustive 744x744 authentication tests using the i-vector modeling tool in [23]. In addition, we further reduce the equal error rates (EERs) by sensor fusion using the average score from the two modalities. The authentication results are plotted in Figure 4. The normalization effect in cosine similarity GDIs appears to be beneficial as they outperform inner product GDIs for both sensor modalities and also for the fusion case.

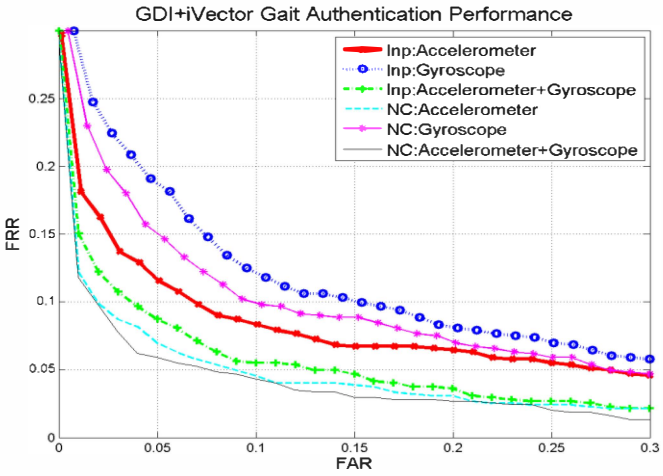

Figure 4. I-vector gait authentication results on the 744-subject Osaka University gait dataset, using inner product GDIs (Inp) and cosine similarity GDIs (NC) from accelerometer, gyroscope and sensor fusion.

We also compare the performances of the proposed algorithms to four existing gait authentication algorithms. As shown in Table 2, our novel GDI+i-vector approach to gait authentication has resulted in significant lower EERs, compared with recently published results on the same data set of 744 subjects, using the same training and testing subsets.

Approach	Sensor modality		
	Acce.	Gyro.	Fused
Gafurov et al. [11]	15.8[21]	NA	NA
Derawi et al. [7]	14.3[21]	NA	NA
Liu et al. [19]	14.3[21]	NA	NA
Ngo et al [21]	13.5[21]	20.2[21]	NA
Inp GDI + i-vector	8.9	11.3	7.1
NC GDI + i-vector	6.8	10.9	5.6

Table 2. Gait authentication performance (EER in %) on the Osaka Univ. gait dataset containing 744 subjects. We compare EERs the proposed algorithm (bottom two rows: using inner product GDIs (Inp GDI) and cosine similarity GDIs (NC GDI) combined with i-vector modeling) with those of four published algorithms (Top four rows, as reported in [21], Table 2) using the same dataset.

6. Conclusions and future work

We have proposed a novel invariant gait representation called gait dynamics images for accelerometer and gyroscope sensory data. On the one hand, GDIs are robust to variations in sensor orientation. GDIs are also invariant to symmetry transforms of the motion measurements. As the bilateral symmetry in human bodies often result in symmetric locomotion for the left and right side of the body, it is possible to match GDIs computed using a device placed in one pocket to GDIs computed from a device carried in a corresponding pocket on the other side. These invariant properties of GDIs greatly relax the sensor placement restrictions for realistic mobile gait biometrics. On the other hand, GDIs are highly informative and discriminative by encoding fine scale intrinsic interactions and complex dynamics within gait cycles to enable high performance gait authentication for a large user population. With these two advancements combined, GDIs offer mobile device users a promising gait representation allowing for robust and accurate gait biometrics in their daily lives.

We have applied the i-vector approach, commonly used in speaker recognition to recover identity information from noisy voice signals, to extract gait identity using GDIs. Gait biometrics performance studies on both the McGill Univ. gait dataset and the Osaka Univ. gait dataset have shown the advantages and superiority of our approach compared to existing gait biometrics algorithms.

The major challenge for mobile gait biometrics is to ensure that they work reliably in an unconstrained environment, just as for other biometrics modalities including face recognition, fingerprinting, iris recognition, and voice identification [14]. An imperative need is to overcome the data dependency on sensor placement. Inertial sensors in phones capture local motion when worn on the body. These motion patterns are likely different

when the phones are carried in separate pockets. Even when the phone is placed at the same location, the motion measurements differ depending on the orientation of the phone. GDIs provide invariant gait representation for sensors placed at approximately the same location, regardless of orientation. Their invariance to symmetry transforms (and concatenations of rotation transforms and symmetry transforms) also allows for consistent signature extraction when the device is placed in either one of two laterally symmetric pockets. The proposed work moves gait biometrics one step forward from existing laboratory studies towards more widespread and casual use in people's daily lives. However, we have yet to address motion variations caused by location differences that are not laterally symmetric. We will explore comprehensive training and advanced machine learning algorithms such as manifold learning or knowledge transfer to further improve the accuracy of gait biometrics.

Acknowledgements

We would like to thank Thanh Trung Ngo and Jordan Frank for providing the gait datasets used in the performance study, and for answering our questions. We would also like to thank the anonymous reviewers for their constructive suggestions.

References

[1] K. Aminian, B. Najafi, C. Büla, P-F. Leyvraz, and P. Robert. Spatio-temporal parameters of gait measured by an ambulatory system using miniature gyroscopes. *Journal of biomechanics* 35, no. 5 (2002): 689-699.

[2] M. Bachlin, J. Schumm, D. Roggen, and G. Toster, Quantifying gait similarity: user authentication and real-world challenge. *Advances in Biometrics*, 2009.

[3] L. Bao, and S. Intille. Activity recognition from user-annotated acceleration data. *Pervasive Computing*, pp. 1-17. Springer Berlin Heidelberg, 2004.

[4] R.G. Cutler and L.S. Davis, "Robust real-time periodic motion detection, analysis and applications," *IEEE Trans. Pattern Analysis and Machine Intelligence*, 22(8), 2000.

[5] N. Dehak, P.J. Kenny, R. Dehak, P. Dumouchel, and P. Ouellet, FrontEnd Factor Analysis for Speaker Verification. *IEEE Trans. Audio, Speech, and Lang. Proc.*, 19(4), 2011.

[6] M.O. Derawi. Accelerometer-based gait analysis, a survey. *Norwegian Information Security Conf.*, pp. 33–44, 2010.

[7] M.O. Derawi, P.Bours, and K.Holien. Improved cycle detection for accelerometer based gait authentication. 6th IEEE Int'l Conf. *Intelligent Information Hiding and Multimedia Signal Processing (IIH-MSP),* 2010.

[8] J. Frank, S. Mannor, and D. Precup, Data Sets: Mobile Phone Gait Recognition Data (http://www.cs.mcgill.ca/~jfrank8/data/gait-dataset.html), 2010.

[9] J. Frank, S. Mannor, J. Pineau, and D. Precup, Time Series Analysis Using Geometric Template Matching, *IEEE Trans. Pattern Analysis and Machine Intelligence*, 35(3), 2013.

[10] D. Gafurov, K. Helkala, and T. Søndrol. Biometric gait authentication using accelerometer sensor. *JCP*, 1(7), 2006.

[11] D. Gafurov, E. Snekkenes, P. Bours, Improved gait recognition performance using cycle matching, IEEE 24th Int'l Conf. Advanced Information Networking and Applications Workshops (WAINA), 2010.

[12] T. Iso and K. Yamazaki, Gait analyzer based on a cell phone with a single three-axis accelerometer, the *8th Conf. on Human-computer interaction with mobile devices and services*, pp. 141-144, 2006.

[13] A. K. Jain, R. Bolle, and S. Pankanti (editors), Biometrics: Personal Identification in Networked Society, Kluwer Academic Publishers, 1999.

[14] A. K. Jain, S. Pankanti, S. Prabhakar, L. Hong, and A. Ross, Biometrics: a grand challenge, *Proc. Int'l Conf. on Pattern Recognition*, vol. 2, pp. 935–942, 2004.

[15] A. Kale, N.Cuntoor, B. Yegnanarayana, A. N. Rajagopalan, and R.Chellappa. Gait analysis for human identification, *Audio-and Video-Based Biometric Person Authentication*, pp. 706-714. Springer Berlin Heidelberg, 2003.

[16] T. Kobayashi, K. Hasida, and N. Otsu. Rotation invariant feature extraction from 3-d acceleration signals. *Int'l Conf. on Acoustics, Speech, and Signal Processing*, 2011.

[17] J. R. Kwapisz, G. M. Weiss, and S. A. Moore. Cell phone-based biometric identification. *Biometrics: 4th IEEE Int'l Conf. Theory Applications and Systems (BTAS),* 2010.

[18] L. Lee and W. E. L. Grimson, Gait analysis for recognition and classification. In *Proc. 5th IEEE Int'l Conf. Automatic Face and Gesture Recognition*, pp. 148-155, 2002.

[19] R. Liu, J. Zhou, and X. Hou, A wearable acceleration sensor system for gait recognition, *2nd IEEE Conf. Industrial Electronics and Applications*, 2007.

[20] J. Mantyjarvi, M. Lindholm, E. Vildjiounaite, S.M. Makela, and H. Ailisto, Identifying users of portable devices from gait pattern with accelerometers, *IEEE Int'l Conf. Acoustics, Speech, and Signal Processing*, vol. 2, 2005.

[21] T.T. Ngo, Y. Makihara, H. Nagahara, Y. Mukaigawa, and Y. Yagi, The Largest Inertial Sensor-based Gait Database and Performance Evaluation of Gait Recognition, Pattern Recognition, 47(1), pp. 228-237, Jan. 2014.

[22] G. Pan, Y. Zhang, and Z. Wu. Accelerometer-based gait recognition via voting by signature points. *Electronics letters* 45(22): 1116-1118, 2009.

[23] D. Povey, A. Ghoshal, G. Boulianne, L. Burget, O. Glembek, N. Goel, M. Hannemann, P. Motlicek, Y. Qian, P. Schwarz, J. Silovsky, G. Stemmer, and K. Vesely, The Kaldi speech recognition toolkit, *Proc. IEEE ASRU*, 2011.

[24] W. Premerlani and P. Bizard, Direction cosine matrix IMU: theory. http://gentlenav.googlecode.com/files/DCMDraft2.pdf

[25] S. Sarkar, P.J. Phillips, Z. Liu, I.R. Vega, P.Grother, and K. W. Bowyer, The humanID gait challenge problem: Data sets, performance, and analysis. *IEEE Trans.Pattern Analysis and Machine Intelligence, 27*(2):162-177, 2005.

[26] S. Sprager, A cumulant-based method for gait identification using accelerometer data with principal component analysis and support vector machine, *Sensors, Signals, Visualization, Imaging, Simulation and Materials*, pp. 94-99, 2009.

[27] F. Juefei-Xu, C. Bhagavatula, A. Jaech, U. Prasad, M. Savvides, Gait-ID on the move: Pace independent human identification using cell phone accelerometer dynamics, *IEEE Fifth Int'l Conf. on Biometrics: Theory, Applications and Systems (BTAS)*, pp. 8 – 15, 2012.